Eur. Phys. J. Special Topics **150**, 61–66 (2007)

DOI: 10.1140/epjst/e2007-00267-7

THE EUROPEAN PHYSICAL JOURNAL SPECIAL TOPICS

Neutron excess nuclei of hydrogen and helium at ACCULINNA

G.M. Ter-Akopian[1], A.S. Fomichev[1], M.S. Golovkov[1], L.V. Grigorenko[1], S.A. Krupko[1], Yu.Ts. Oganessian[1], A.M. Rodin[1], S.I. Sidorchuk[1], R.S. Slepnev[1], S.V. Stepantsov[1], R. Wolski[1,2], A.A. Korsheninnikov[3,a], E.Yu. Nikolskii[3,b], P. Roussel-Chomaz[4], W. Mittig[4], V.A. Kuzmin[5], B.G. Novatskii[5], and D.N. Stepanov[5]

[1] Joint Institute for Nuclear Research, 141980 Dubna, Russia
[2] The Henryk Niewodniczański Institute of Nuclear Physics, Kraków, Poland
[3] RIKEN, 2-1 Hirosawa, Wako, Saitama 351-0198, Japan
[4] GANIL, BP. 5027, 14076 Caen Cedex 5, France
[5] The Kurchatov Institute, Kurchatov sq. 1, 123182 Moscow, Russia

Received: January 31, 2007

Abstract. Attempt to observe a ^{7}H resonance produced in the reaction ^{2}H(^{8}He,^{3}He)^{7}H resulted only in setting a limit $d\sigma/d\Omega \leq 20\,\mu$b/sr for the reaction exit channel which could populate a resonance lying between 0 and 3 MeV above the ^{7}H decay threshold. The quasi-free scattering of the α core bound in ^{6}He was explored keeping in mind the possible study of the cluster structure of this halo nucleus. For the first time coincident particles emitted in the ^{4}He(^{6}He, 2α)nn reaction were detected in wide angular ranges giving a wide kinematical range of the measured angular and momentum distributions. The contribution of processes, competing with QFS in the $\alpha + \alpha + n + n$ output channel, was considerably suppressed by the selection of events with $E_{\alpha 1(2)-nn} > 10$ MeV. A number of experimental distributions, relevant to the reaction mechanism and to the ^{6}He structure, were compared with the results of MC simulations based on the PWIA formalism. The PWIA predictions showed consistency with the experimental data.

PACS. 25.10.+s Nuclear reactions involving few-nucleon systems – 24.50.+g Direct reactions – 25.60.-t Reactions induced by unstable nuclei – 27.30.+n Properties of specific nuclei listed by mass ranges: $6 \geq A \geq 19$ – 25.60.Je Transfer reactions

1 Introduction

Drip-line nuclei of hydrogen and helium make an essential part of the Dubna radioactive beam (RIB) research accomplished with low energy ($E \leq 40$ MeV/amu) beams of radioactive nuclei delivered by the RIB separator ACCULINNA [1,2]. The finding of a two-neutron exchange process resulting in a large cross section value for the backward direction ^{6}He + ^{4}He elastic scattering at $E_{lab} = 25$ MeV/amu made the first experimental proof of the "di-neutron" configuration in ^{6}He [3]. The known extended distribution of neutron matter in ^{6}He was explored with the ^{6}He + ^{1}H elastic and inelastic scattering measured in a broad angular range with a 24.5 MeV beam of ^{6}He nuclei [4]. Data acquired about elastic scattering and 1n and 2n transfer reactions observed for the ^{6}He + ^{1}H system testified to a large "di-neutron" spectroscopic factor in ^{6}He and a low probability for a t+t clustering in its structure [5]. A similar study made for the ^{8}He + ^{1}H reaction resulted in the estimation of spectroscopic factors for the ^{6}He(0^+g.s.) and ^{6}He(2^+) subsystems in ^{8}He and in the observation of a ^{5}H + t clustering in the ^{8}He structure [6,7]. Search for a four-neutron exchange in the ^{8}He + ^{4}He reaction fixed only an upper limit of 1 μb/sr for the cross section of backward direction elastic scattering of 25 MeV/amu ^{8}He nuclei [6].

Due to their inherent transparency and not too low cross sections, transfer reactions induced by RIBs were proven to be effective in the study of resonance states of particle unstable drip-line nuclei. Cryogenic tritium targets [8] and a 58 MeV beam of ^{3}H nuclei accelerated at the Dubna U-400M cyclotron [9] played essential role in this work, alongside with the ^{6}He and ^{8}He beams delivered by ACCULINNA. The energy and width of the ^{4}H ground state (g.s.) resonance were finally determined in a complete kinematic study made for the transfer reactions ^{2}H(t,p)^{4}H and ^{3}H(t,d)^{4}H [10]. The ^{5}H puzzle was resolved in experiments where the ground state resonance of this nuclear system was investigated using the ^{1}H(^{6}He, ^{2}He)^{5}H [11] and ^{3}H(t,p)^{5}H [12,14] reactions. Complete kinematic measurements and spin alignment, obtained in conditions of "zero angle" geometry realized in experiments of [13,14], were essential for the revelation of the $1/2^+$

[a] *Present address:* The Kurchatov Institute, Kurchatov sq. 1, Moscow, 123182 Russia
[b] *On leave from:* The Kurchatov Institute, Kurchatov sq. 1, Moscow, 123182 Russia

g.s. resonance and the $3/2^+$-$5/2^+$ doublet of excited resonance states in the ^{5}H continuum populated in the ^{3}H(t,p)^{5}H reaction. It is worth noting that a T = 3/2 isobaric analog state of the ^{5}H g.s. was for the first time obtained in the ^{5}He spectrum populated in the transfer reaction ^{2}H(^{6}He, ^{3}He)^{5}He [15].

These results give us inspiration to employ RIB transfer reactions in order to get even more neutron-excess nuclei of hydrogen and helium. Quite recently we completed an experiment in Dubna combining the conditions necessary for detecting the formation of ^{7}H and ^{9}He nuclei emerging as products in the ^{8}He + ^{2}H reaction. Section 2 gives an account of our attempts to observe the ^{7}H nucleus in this experiment. Results derived for ^{9}He are the subject of other paper presented at this conference [16].

Exploratory study was undertaken for the α, 2α knock-out occurring when a helium target was bombarded with a 25 MeV/amu ^{6}He beam. Conditions adopted in this experiment facilitated the observation of quasi-free scattering (QFS) of helium target nuclei from the α-cluster core of the ^{6}He halo nucleus. These results are presented in section 3.

2 Search for ^{7}H manifestation in the ^{8}He + ^{2}H reaction

In [17] we revisited the long-standing issue of the ^{7}H nucleus (see [18] and references in [17]) setting an upper limit of 3 nb/sr for the cross section of the reaction ^{2}H(^{8}He, ^{3}He)^{7}H which could populate a (hypothetical) quasi stable ($T_{1/2} \geq 1$ ns) resonance state in ^{7}H. One could not *a priory* exclude such a long life time for ^{7}H without checking this experimentally because, most likely, this nucleus undergoes an unique decay – the four neutron emission (five-body decay). Estimates [17] show that most likely the width of the ^{7}H g.s. resonance will be less than 1 MeV, if its decay energy is less than 2–3 MeV. In the experiment discussed here, we made an attempt to observe the ^{7}H resonance which could come to light in the missing mass spectrum derived from the kinematic characteristics measured for the ^{3}He nuclei emitted in the ^{2}H(^{8}He, ^{3}He)^{7}H reaction.

A 34 MeV/amu primary beam of ^{11}B accelerated by the U-400M cyclotron bombarded the production target of ACCULINNA (Be, 370 mg/cm^2). At a typical primary beam intensity making 4 pμA a secondary ^{8}He beam with intensity of 2×10^4 s^{-1} was separated and delivered to the deuterium target. The part of the admixture flux of tritons in the secondary ^{8}He beam was less than 10%. The target was a gas cell filled with deuterium at 1020 mPa and cooled down to 25 K. The 4 mm thick target cell was supplied with 6 μm stainless steel windows.

Slow ^{3}He nuclei escaping from the target in the forward direction were detected by a telescope composed of a front array of 8 sector type, 40 μm thick Si detectors followed by an annular 300 μm Si detector having an active area of the outer and inner diameters of 82 mm and 32 mm, respectively. It was segmented in 16 rings on one side and 16 sectors on the other side providing a good position resolution. The 40 μm array matched the active area of the annular detector. The telescope was installed 100 mm downstream of the target. The ΔE-E particle identification, provided by the telescope, was essential since the overwhelming majority of detected charged particles were tritons and ^{4}He nuclei. This background was considerably suppressed by taking a condition that the ^{3}He nuclei emitted in the ^{2}H(^{8}He,^{3}He)^{7}H reaction were detected in coincidence with the the ^{3}H nuclei resulting from the ^{7}H decay.

The ^{3}H nuclei were detected by a Si-CsI telescope mounted in air just behind the exit window of the vacuum chamber, at a distance more than 50 cm from the target. The telescope consisted of two $1 \times 60 \times 60$ mm Si detectors and a wall of sixteen $1.5 \times 2 \times 2$ cm CsI crystals coupled with photodiodes. The Si detectors were segmented in 32 strips both in horizontal and vertical directions, providing a good position resolution and particle identification by the ΔE-E method (together with the following thick CsI detectors). The telescope area was sufficient to provide a good efficiency for the detection of the ^{3}H nuclei in coincidence with the ^{3}He reaction products in the whole measured range of the ^{7}H missing mass spectrum. The energy of the ^{8}He beam in the target median plane was $\sim$25 MeV/amu. The energy spread and angular divergence of the beam and the diameter of the beam spot on the target were 8.5%, 0.23°, and 20 mm, respectively. Two plastic scintillation counters installed on a 785 cm base provided the time-of-flight (TOF) measurements for the beam particles. The overall time resolution was 0.8 ns. The ^{8}He nuclei in the beam were recognized individually according to their TOF and energy loss (ΔE) in plastic. Beam tracking was made by two multiwire proportional chambers installed 26 and 80 cm upstream of the target. Each chamber had two perpendicular planes of wires with a 1.25 mm pitch. Energy resolution in the ^{7}H missing mass spectrum was estimated by Monte-Carlo (MC) simulation taking into account all experimental details. It was found to be 0.6 MeV (FWHM). Measurements made for the ^{2}H(^{8}He,^{3}He)^{7}H reaction covered a range of the reaction center-of-mass (CM) angles $\theta_{CM} = 9° - 21°$.

After two weeks of continuous bombardments 2×10^{10} ^{8}He nuclei passed through the deuterium target. A ^{7}H missing mass spectrum resulting from the detected ^{3}He-^{3}H coincidence events is presented in figure 1, panel B. Panel A in figure 1 shows the ^{7}H spectrum derived from the data collected for single ^{3}He nuclei. Evidently, the more rich pattern seen in the spectrum of panel A was due to the ^{4}He background which partly could fall into the ^{3}H locus on the ΔE-E identification plot. From the few events observed in the spectrum of figure 1, panel B, only a cross section limit $d\sigma/d\Omega \leq 20$ μb/sr follows for the reaction ^{2}H(^{8}He,^{3}He)^{7}H populating a resonance lying between 0 and 3 MeV above the ^{7}H decay threshold.

3 QFS in the ^{4}He(^{6}He,2α)2n reaction

Quasi-free scattering of nucleons and clusters bound in nuclei is acknowledged as a tool for the nuclear structure study (see e.g. [19–21]). Along with the use of

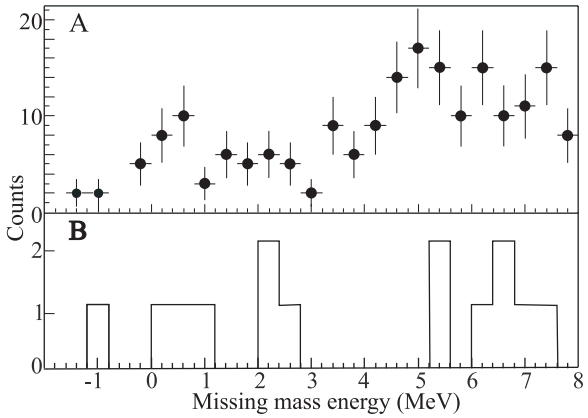

Fig. 1. Missing mass spectrum of ^{7}H derived from the ^{2}H(^{8}He,^{3}He)^{7}H reaction data. A - spectrum obtained from the detected single ^{3}He nuclei, B - spectrum obtained from the ^{3}He-^{3}H coincidence events.

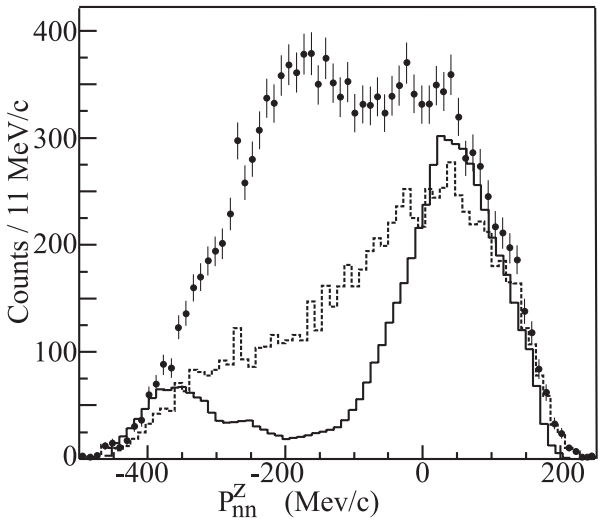

Fig. 2. Distribution in momentum component P^{Z}_{nn} observed in the reaction ^{4}He(^{6}He,2α)nn. Points with error bars show the total distribution. The distributions of events selected by the $\alpha-\alpha$ CM scattering angle $\theta_{CM} = 60°$–$120°$ and by the values of $E_{\alpha 1(2)-nn} > 10$ MeV are shown, respectively, by the dashed and solid line histograms. (See explanations in text.)

electron beams, QFS induced by beams of protons and α particles was studied extensively. Momentum distributions and spectroscopic factors were extracted in these experiments for the knocked-out particles. Usually, the remaining third body (spectator) was either nuclear stable or it was found in a quasi-stationary state. The data were mostly analyzed using Plane Wave Impulse Approximation (PWIA) and better correspondence between experimental data and theory predictions was achieved at higher collision energies. The Distorted Wave Impulse Approximation (DWIA) was shown [22] to be more reliable in getting correct values for spectroscopic factors even from the QFS data acquired with the use of rather low energy beams. In [23] the QFS reaction ^{6}Li(α, 2α)d was investigated at ^{4}He beam energies around 100 MeV. The authors analyzed their data by means of PWIA and DWIA showing that the two approaches lead to quite similar conclusions about the momentum distribution of the α cluster in the ^{6}Li nucleus and both results were in accord with the wave function of ^{6}Li given by theory. Most likely, the reason why the PWIA analysis appeared to be correct in this case is associated with the small binding energy of the α cluster in ^{6}Li. Such a situation seems to be even more reasonable for the weakly bound drip-line nuclei.

To check this assumption we made a test experiment dedicated to the observation of the QFS of the ^{6}He α core showing up in the ^{4}He(^{6}He,2α)nn reaction. It was tempting to know from this experiment whether the study of QFS can be used for direct observations of three-body correlations specific for the ground state of Borromean nuclei. ^{6}He is a convenient object for such a study because one can believe that its three-body wave function (WF) is well established in theory [24]. The peculiarity of the ^{4}He(^{6}He,2α)nn reaction consists in the lack of a bound state for the two neutrons becoming free after the knock out of the ^{6}He α core. Similar situation occurred when the QFS reactions ^{6}Li(α,2α)pn and ^{6}Li(p,pα)pn were investigated [25,26]. These experiments were performed in coplanar geometry with the use of small-aperture detectors.

We studied the reaction ^{4}He(^{6}He,2α)nn at a ^{6}He beam energy of 25A MeV/amu. The secondary beam of ^{6}He nuclei with intensity of 2×10^{4} s^{-1} bombarded a helium gas target cooled down to 16 K. The target thickness was 2×10^{20} cm^{-2}. The beam diagnostic array was such as outlined in section 2. The coincident two α particles emitted from the target in angular ranges of 15°–55° were detected by two position sensitive ΔE-E telescopes installed symmetrically in respect to the beam direction. Each telescope had a pair of Si strip detectors (one of these detectors had a thickness of 70 μm and another one was 1 mm thick). Behind of this pair, a 6.2 mm Si(Li)detector was installed in each telescope. The measured α particle energies and angles allowed us to calculate relative momentum values, $P_{(n-n)}$, observed for the two spectator neutrons in their CM system, and momentum vectors $\mathbf{P}_{nn}$ characterizing the motion of their CM in the projectile reference frame. Resolution attained in the momentum values was about 15 MeV/c. With Z axis chosen to coincide with the projectile trajectory, the polar and azimuthal angles of momentum vector $\mathbf{P}_{nn}$ were determined with errors of $\leq 1.5°$. A quite low background level was observed in a run made with empty target.

Two bumps are seen in figure 2 showing the P^{Z}_{nn} distribution observed in the reaction ^{4}He(^{6}He,2α)nn.[1] Spectator neutrons originating from "real" $\alpha-\alpha$ QFS should be found in the event group centered around the $P^{Z}_{nn} = 0$ point. The maximum rising nearby the $P^{Z}_{nn} = -200$ MeV/c point is made by different processes, e.g. the 1n or α transfer from ^{6}He to ^{4}He, or inelastic scattering occurring in the collisions of ^{6}He projectiles with ^{4}He nuclei. The contribution of these reaction channels extends rather far to the right side of the $P^{Z}_{nn} = -200$ MeV/c

[1] P^{Z}_{nn} is longitudinal (Z) component of momentum $\mathbf{P}_{nn}$.

point. The tail of this contribution presents near P^Z_{nn}=0. The elimination of small $\alpha-\alpha$ CM scattering angles (taking $\theta_{\alpha-\alpha} = 60°-120°$) considerably reduced the part of these interfering processes. Their contribution was also suppressed by the event selection made with the choice of events characterizes with large values of the energy of relative motion observed in the subsystems $\alpha 1-$nn and $\alpha 2-$nn. The distribution obtained with a choice of $E_{\alpha 1(2)-nn} > 10$ MeV is presented in figure 2. At this choice, the overall contribution of the interfering reaction channels in the obtained spectra was well described as a four-body phase space (PS).

To analyze these data, we performed complete MC simulations using a standard PWIA factorization for the transition matrix:

$$\left(\frac{\mathrm{d}\sigma}{\mathrm{d}\Omega}\right)^{QFS}_{\alpha-\alpha} \sim S^2(\mathbf{P}_{n-n}, \mathbf{P}_{\alpha-nn}) \left(\frac{\mathrm{d}\sigma}{\mathrm{d}\Omega}\right)_{\alpha-\alpha} \times F_{PS} dE_{n-n} dE_{\alpha-\alpha} d\Omega_{\alpha\alpha-nn} d\Omega_{n-n}, \quad (1)$$

where $F_{PS} = \sqrt{E_{n-n}E_{\alpha-\alpha}(E_0 + Q - E_{n-n} - E_{\alpha-\alpha})}$ is a phase space factor that accounts for energy conservation, $E_0 = E_{n-n} + E_{\alpha-\alpha} + E_{\alpha\alpha-nn} - Q$ is the CM energy of the whole $\alpha-\alpha-n-n$ system ($E_{\alpha\alpha-nn}$ stands for the energy of relative motion of the $\alpha\alpha$ and nn centers-of-mass). The $\alpha-\alpha$ elastic scattering cross section, $(\frac{\mathrm{d}\sigma}{\mathrm{d}\Omega})_{\alpha-\alpha}$, was calculated for the relative energy $E_{\alpha-\alpha}$ measured in the reaction exit channel. This implied the use of the final-state energy prescription.

Due to the large acceptance provided by the detection system the two α particles were observed in a wide range of their relative energy $E_{\alpha-\alpha} = (5-60)$ MeV and the observed scattering angle $\theta_{\alpha-\alpha}$ covered a range of (30°–150°). The dependence of cross-section $(\frac{d\sigma}{d\Omega})_{\alpha-\alpha}$ on $E_{\alpha-\alpha}$ and $\theta_{\alpha-\alpha}$ was derived from the known set of phase shifts measured in a proper energy range.

Function $S(\mathbf{P}_{n-n}, \mathbf{P}_{\alpha-nn})$, entering into equation 1, contains nuclear structure information relevant to ^{6}He.[2] Taking into account the n-n final state interaction (FSI), this function was calculated as

$$S(\mathbf{P}_{n-n}, \mathbf{P}_{\alpha-nn}) = \int \mathrm{d}\mathbf{r}_{n-n}\mathrm{d}\mathbf{r}_{\alpha-nn}\psi^*_{n-n}(\mathbf{P}_{n-n}, \mathbf{r}_{n-n}) \times \; e^{-i\mathbf{P}_{\alpha-nn}\mathbf{r}_{\alpha-nn}}\psi_{6He}(\mathbf{r}_{n-n}\mathbf{r}_{\alpha-nn}), \quad (2)$$

where $\psi_{6\mathrm{He}}(\mathbf{r}_{n-n}\mathbf{r}_{\alpha-nn})$ is the three-body wave function of ^{6}He [24].

Joint momentum distribution $S^2(\mathbf{P}_{n-n}, \mathbf{P}_{\alpha-nn})$ was extracted from the measured data with the use of equation (1). The data were selected with the simultaneous imposition of the two criteria presented in figure 2. Additionally, condition $P^Z_{nn} \geq 0$ MeV/c was imposed. The obtained experimental distribution is shown in figure 3 together with a MC simulation made with the use of equation (2) and taking into account the real experimental conditions.

[2] In Jacobi co-ordinates, adopted in the three-body model of Borromean nuclei, the momenta $\mathbf{P}_{n-n}$ and $\mathbf{P}_{\alpha-nn}$ have conventional notations $\mathbf{p}_x$ and $\mathbf{p}_y$, respectively.

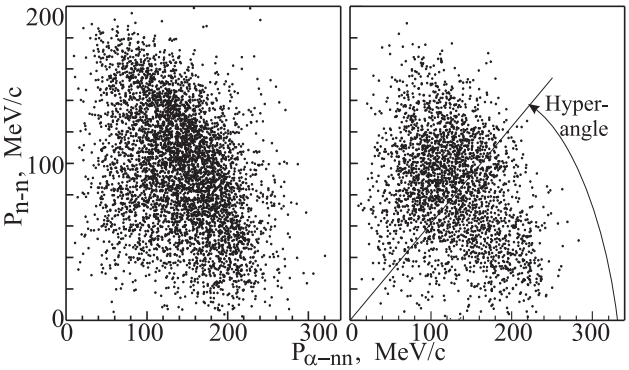

Fig. 3. Joint momentum distribution $S^2(\mathbf{P}_{n-n}, \mathbf{P}_{\alpha-nn})$ extracted from the experimental data (left panel) and obtained by MC simulation (right panel). Drawing in the right panel explains the notion of hyperangle used to characterize similar distributions in the three-body model. (See explanations in text.)

The two distributions shown in figure 3 are similar in the widths of their projections to the axes P_{n-n} and $P_{\alpha-nn}$. However, one sees also differences between the two patterns, perhaps, arising from the contribution of reaction channels, different from QFS. To check whether the QFS part is considerable in the experimental distribution (see figure 3, left panel) we fitted a set of experimentally measured distributions by the sums of MC simulations made for the QFS and PS spectra. Some of these distributions are shown in figure 4 together with the fitting results. One can make sure that the fits provide a good description of the experimental distributions.

This inference seems to be not trivial in the light of the fact that the process of QFS was treated in the framework of the model based on assumptions inherent to equation (1). It is remarkable that the final state energy prescription, employed for the calculation of $(\frac{\mathrm{d}\sigma}{\mathrm{d}\Omega})_{\alpha-\alpha}$, lead to a reasonably good fit to the experimental $\theta_{\alpha-\alpha}$ distribution obtained as a sum of QFS events characterized by so different values of final state energy $E_{\alpha-\alpha}$ (see the lower two panels in figure 4).

In figure 5 we show three distributions in $\theta_{\alpha-\alpha}$ obtained from different cuts made in $E_{\alpha-\alpha}$. These spectra were built from the bulk of detected events selected to satisfy conditions $E_{\alpha 1(2)-nn} > 10$ MeV and $P_{n-n} > 100$ MeV/c. It is seen from the upper right panel in figure 4 that the choice of events with $P_{n-n} > 100$ MeV/c is associated with a relative strengthening of the QFS part in the data. Strong variations visible in the angular dependencies presented in figure 4 are all due to the behavior of the QFS cross section (the phase-space spectra are smooth). The excellent fits made to these experimental spectra makes us confident that the effect of QFS has been well revealed in this experiment.

Summarizing, we note that in our experiment the QFS of the α core bound in ^{6}He was explored keeping in mind the possible study of the cluster structure of this halo nucleus. The possible use of QFS measurements for revealing momentum correlations specific for three-body Borromean nuclei was the subject of our interest. The

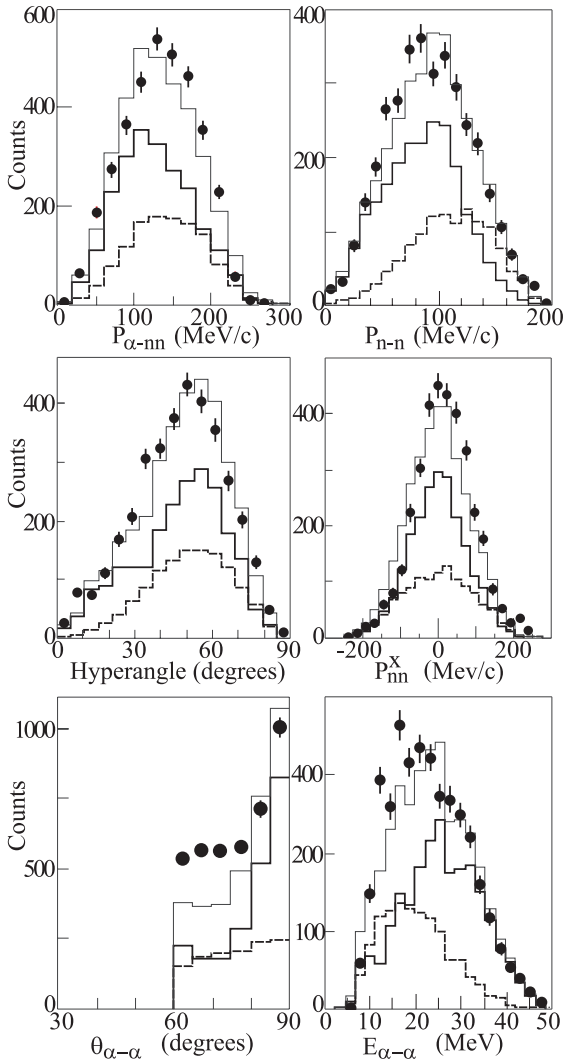

Fig. 4. Result of fits made to six distributions obtained from the experimental data. The two upper panels present the two projections of the distribution shown in figure 3 (left panel). In the middle panels the event distributions are shown in function of hyperangle (see definition in figure 3, right panel) and P^X_{nn}, the transverse projection of the recoil momentum $\mathbf{P}_{nn}$. Event distributions in $\alpha-\alpha$ CM scattering angle $\theta_{\alpha-\alpha}$ and energy $E_{\alpha-\alpha}$ are shown in bottom. Points with error bars show the experimental data. The fit results obtained for the QFS and PS spectra are shown by histograms drawn by thick solid line and dashed line, respectively. Thin-line histograms show the sums of these contributions.

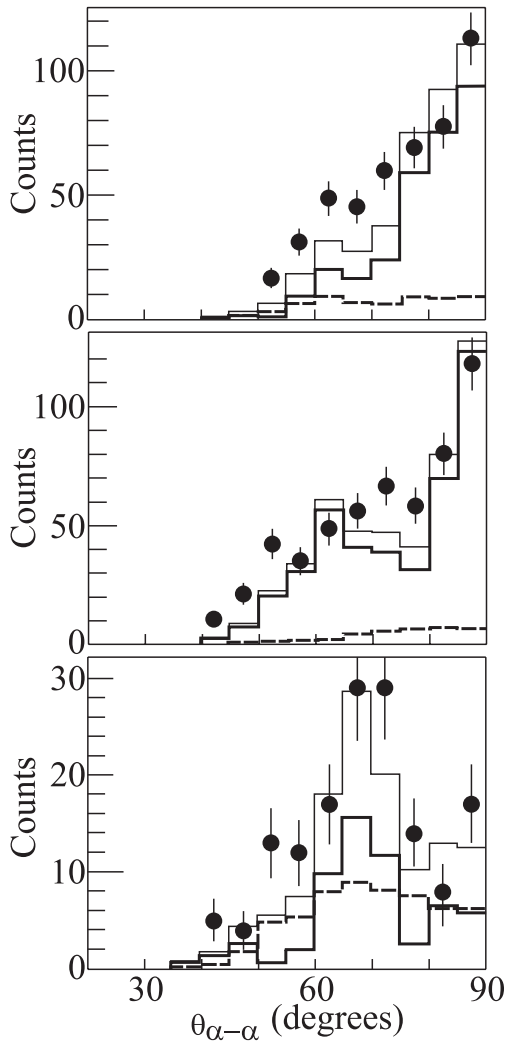

Fig. 5. Angular dependence obtained for QFS events with values of $E_{\alpha-\alpha}$ chosen to be 15–20, 30–35 and 45–50 MeV. Experimental data were selected to satisfy conditions $E_{\alpha 1(2)-nn} > 10$ MeV and $P_{n-n} > 100$ MeV/c. (See notations in caption to figure 4.)

three-body WF of ^{6}He is believed to be well established in theory and a comparison of theoretical predictions with experimental data could be a good test for the use of QFS for the study of clustering states in halo nuclei.

For the first time coincident particles emitted in the ^{4}He(^{6}He,2α)nn reaction were detected in wide angular ranges giving a wide kinematical range of the measured angular and momentum distributions. The contribution of processes, competing with QFS in the $\alpha+\alpha+n+n$ output channel, was considerably suppressed by the selection of events with $E_{\alpha 1(2)-nn} > 10$ MeV. This condition provided a reliable separation of events corresponding to QFS. A number of experimental distributions, relevant to the reaction mechanism and to the ^{6}He structure, was compared with the results of MC simulations based on the PWIA formalism. The PWIA predictions showed consistency with the experimental data. Due to the n-n FSI such a pronounced peculiarity of the ^{6}He WF as Pauli focusing was not observed. One should note that the n-n FSI is the only distorting factor involved in the data analysis. We assume that the influence of the n-n FSI will be less significant at higher energies of bombarding ^{6}He nuclei.

The ratio of the cross-section $(\frac{d\sigma}{d\Omega})_{\alpha-\alpha}$, emerging from our data, to the cross section value of the free $\alpha-\alpha$ elastic scattering was found to be constant in energy ranges $10 < E_{\alpha-\alpha} < 50$ MeV and $0 < E_{n-n} < 40$ MeV. The angular distributions of quasi-free $\alpha-\alpha$ scattering measured for different energies $E_{\alpha-\alpha}$ were well reproduced

by MC simulation while the relative values of the four-body breakup and $\alpha - \alpha$ elastic scattering cross-sections varied by more than two orders of magnitude in the energy and angular ranges allowed by the used detector array.

This work was supported by the Russian Foundation for Basic Research grants 05-02-16404, and 05-02-17535 and by the INTAS grants 03-51-4496 and 03-54-6545. LVG acknowledge the financial support from the Royal Swedish Academy of Science and Russian Ministry of Industry and Science grant NS-1885.2003.2.

References

1. A.M. Rodin et al., Nucl. Instrum. Meth. B **126**, 236 (1997)
2. A.M. Rodin et al., Nucl. Instrum. Meth. B **204**, 114 (2003)
3. G.M. Ter-Akopian et al., Phys. Lett. B **426**, 151 (1998)
4. S.V. Stepantsov et al., Phys. Lett. B **542**, 35 (2002)
5. R. Wolski et al., Phys. Lett. B **467**, 8 (1999)
6. R. Wolski et al., Nucl. Phys. A **701**, 29c (2002)
7. G.M. Ter-Akopian et al., Nucl. Phys. A **734**, 295 (2004)
8. A.A. Yukhimchuk et al., Nucl. Instrum. Meth. A **513**, 439 (2003)
9. Yu.Ts. Oganessian et al., Bull. Rus. Acad. Sci. Phys. **66**, 676 (2002)
10. S.I. Sidorchuk et al., Phys. Lett. B **594**, 54 (2004)
11. A.A. Korsheninnikov et al., Phys. Rev. Lett. **87**, 092501 (2001)
12. M.S. Golovkov et al., Phys. Lett. B **566**, 70 (2003)
13. M.S. Golovkov et al., Phys. Rev. Lett. **93**, 262501 (2004)
14. M.S. Golovkov et al., Phys. Rev. C **72**, 064612 (2005)
15. G.M. Ter-Akopian et al., Eur. Phys. J. A **25**, 315 (2005)
16. M.S. Golovkov et al. (this conference); M.S. Golovkov et al., nucl-ex/0608035
17. M.S. Golovkov et al., Phys. Lett. B **588**, 163 (2004)
18. A.I. Baz' et al., *Light and Intermediate Mass Nuclei Near the Border of Nuclear Stability* (Nauka, Moscow, 1972) (in Russian)
19. P.G. Roos et al., Phys. Rev. C **15**, 69 (1977)
20. C.W. Wang et al., Phys. Rev. C **21**, 1705 (1980)
21. G. Jacob et al., Rev. Mod. Phys. **38**, 121 (1966)
22. N.S. Chant, P.G. Roos, Phys. Rev. C **15**, 57 (1977)
23. A. Okihana et al., Nucl. Phys. A **549**, 1 (1992)
24. B.V. Danilin et al., Yad. Fiz. **48**, 1206 (1988)
25. R.F. Warner et al., Nucl. Phys. A **503**, 161 (1989)
26. R.F. Warner et al., Phys. Rev. C **42**, 2143 (1990)